

PePNet: A Periodicity-Perceived Workload Prediction Network Supporting Rare Occurrence of Heavy Workload

Feiyi Chen, Zhen Qin, Hailiang Zhao[†], Shuiguang Deng[†]
Zhejiang University
 {chenfeiyi,zhenqin,hliangzhao,dengsg}@zju.edu.cn

Abstract—Cloud providers can greatly benefit from accurate workload prediction. However, the workload of cloud servers is highly variable, with occasional heavy workload bursts. This makes workload prediction challenging. There are mainly two categories of workload prediction methods: statistical methods and neural-network-based ones. The former ones rely on strong mathematical assumptions and have reported low accuracy when predicting highly variable workload. The latter ones offer higher overall accuracy, yet they are vulnerable to data imbalance between heavy workload and common one. This impairs the prediction accuracy of neural network-based models on heavy workload. Either the overall inaccuracy of statistic methods or the heavy-workload inaccuracy of neural-network-based models can cause service level agreement violations. Thus, we propose PePNet to improve overall especially heavy workload prediction accuracy. It has two distinctive characteristics: (i) A Periodicity-Perceived Mechanism to detect the existence of periodicity and the length of one period automatically, without any priori knowledge. Furthermore, it fuses periodic information adaptively, which is suitable for periodic, lax periodic and aperiodic time series. (ii) An Achilles’ Heel Loss Function iteratively optimizing the most under-fitting part in predicting sequence for each step, which evidently improves the prediction accuracy of heavy load. Extensive experiments conducted on Alibaba2018, SMD dataset and Dinda’s dataset demonstrate that PePNet improves MSE for overall workload by 11.8% on average, compared with state-of-the-art methods. Especially, PePNet improves MSE for heavy workload by 21.0% on average.

Index Terms—Time series forecasting, cloud computation.

I. INTRODUCTION

Accurate workload prediction brings huge economic benefits to cloud providers [1] and many cloud frameworks make real-time adjustments based on the workload prediction results [2]. On the one hand, workload prediction provides meaningful insights to improve the utilization of cloud servers while ensuring the quality of service (QoS) [3] [4]. On the other hand, it can also alarm the forthcoming uncommon heavy workload, thus helping to avoid service level agreement (SLA) violations.

However, the high variability of cloud-server workload [5] [6] makes workload prediction challenging. Statistical methods and neural-network-based methods are two mainstream workload prediction methods. The former ones require the time series to satisfy strong mathematical assumptions and are not robust when predicting highly variable workload [5]. For

TABLE I
PROPORTION OF HEAVY WORKLOAD.

Dataset	Heavy workload proportion
CPU usage of Alibaba’s dataset ¹	15.73%
Memory usage of Alibaba’s dataset	12.89%
Workload of Dinda’s dataset [12]	11.15%

example, the classical statistic method, ARIMA [7], requires the time series to be stationary after difference and shows dissatisfied results when predicting highly variable workload [5]. The neural-network-based methods are more suitable to predict highly variable workloads, but they are vulnerable to data imbalance between heavy workload and common one (i.e. the heavy workload is much more uncommon [8]). To demonstrate this, we present statistics of the heavy workload proportion of different datasets in Tab. I, where the heavy workload is defined as the workload greater than the average workload plus one standard deviation for each machine. It has also been proven that the data imbalance between heavy workload and common workload impairs the former’s accuracy [9]. As an empirical example, Fig. 1(a)-Fig. 1(b) shows the overall prediction accuracy and heavy-workload prediction accuracy of some prevailing methods (ARIMA [7], LSTM with attention (LSTMa) [10], Informer [11], Learning based Prediction Algorithm for cloud workload (L-PAW) [5], LSTM and GRU) on Alibaba2018 dataset, where the heavy-workload predicted error is nearly twice as large as the overall predicted error. The inaccurate prediction will not only reduce the utilization of cloud servers but also bring SLA violations, as it provides wrong information to the scheduler.

To predict overall workload and heavy workload accurately, we propose a **Periodic-Perceived Workload Prediction Network** (PePNet), which supports the prediction of highly variable workload with the rarely-occurring heavy workload. PePNet mainly improves the prediction accuracy in two aspects: 1) using the periodically recurrent patterns to guide the workload prediction and 2) using an *Achilles’ Heel Loss Function*², which pays more attention to the under-fitting part to offset the negative influence of data imbalance.

The existing methods that embed the periodic information

¹<https://github.com/alibaba/clusterdata>

²Achilles’ Heel originates from Greek mythology and is the fatal weakness of the hero Achilles

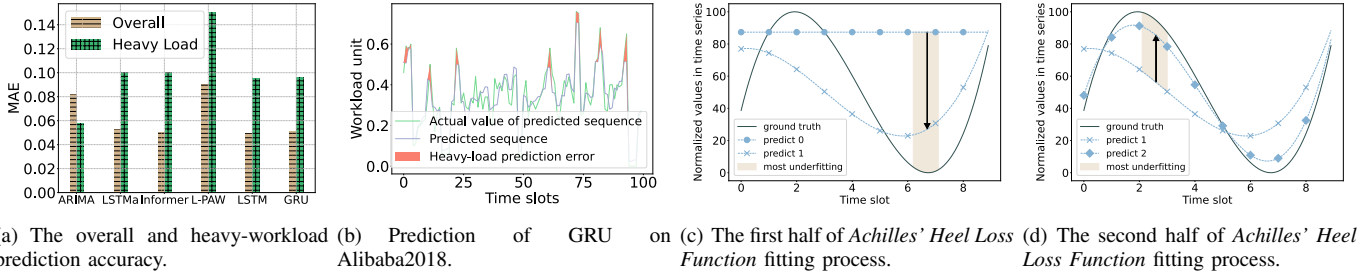


Fig. 1. (a)-(b) Overall workload and heavy workload prediction accuracy. (c)-(d) The fitting process of *Achilles' Heel Loss Function*. (c) In the first half of the process, the most under-fitting part is on the right. (d) After some training iterations, the prediction error on the right diminishes and the most under-fitting part shifts to the left. Then, *Achilles' Heel Loss Function* pays more attention to the left part in this phase.

[13]–[16] are applied to the situations where the periodicity is stable and known (i.e. whether the time series is periodic and the length of a period are fixed and known). However, the cloud environment is complex and highly dynamic. Different servers exhibit different periodicity and even the same server exhibits different periodicity at different time. This calls for a technique that detects periodicity and period length automatically and is capable of manipulating time series with mixed periodicity (i.e. the time series is periodic for some time and aperiodic for the other time). Thus, we propose a *Periodicity-Perceived Mechanism*, which consists of *Periodicity-Mining Module* and *Periodicity-Fusing Module*. The *Periodicity-Mining Module* detects the periodicity and period length and the *Periodicity-Fusing Module* adaptively fuses the periodic information for periodic and aperiodic time series. We mathematically prove the error bound of the periodic information extracted by *Periodicity-Mining Module*. Furthermore, we design an automatic hyperparameter determination method to provide convenience for the training process.

The *Achilles' Heel Loss Function* specifically targets the upper bound of the prediction error, which enables PePNet to strengthen and improve the most vulnerable part of the prediction. At each training step, the *Achilles' Heel Loss Function* picks the most under-fitting part in a predicting sequence and minimizes its prediction error. As shown in Fig.1(c)-1(d), when a kind of pattern is well learned, the most under-fitting part will shift to the position of another pattern. Thus, each part in the predicting sequence is fitted alternatively. This characteristic helps alleviate the problem of overemphasizing sporadic patterns, a limitation that has been observed in many loss functions designed to combat under-fitting issues [17]. In this way, *Achilles' Heel Loss Function* solves the under-fitting problem of heavy load and improves the heavy-load prediction accuracy as well as the overall prediction accuracy.

The main contributions of our work are summarized as:

- We design a Periodicity-Perceived Mechanism, which mines and adaptively fuses the periodic information. Moreover, we mathematically prove an error bound of periodic information extracted by *Periodicity-Mining Module* and propose an automatic hyperparameter determination method for it.
- We have formulated an Achilles' Heel loss function aimed at enhancing the accuracy of heavy workload

prediction and overall prediction performance. This approach effectively mitigates the issue of overemphasizing sporadic patterns, a common limitation faced by many loss functions designed to combat under-fitting problems.

- We conduct extensive experiments on the Alibaba2018, SMD and Dinda's datasets and demonstrate that PePNet improves the heavy-workload prediction accuracy (MSE) by 21.0% on average, while promoting overall prediction accuracy (MSE) by 11.8% on average.

II. METHODOLOGY

Preliminary. The input of data X is divided into three parts, which are denoted by $X_{short}^{enc} \in \mathbb{R}^{I \times d}$, $X_{long}^{enc} \in \mathbb{R}^{M \times d}$, $X_{period} \in \mathbb{R}^{P \times d}$ respectively. The d is the dimension of the feature at each time slot and I, M and P respectively stand for the length of short-term dependent information, long-term tendency information and periodic information. The data division is shown in Fig. 3(a): Y is the ground truth value of predicting workload; X_{short}^{enc} is the nearest workload time series before the predicting part and shows high relevance to predicting workload; X_{long}^{enc} is a bit longer workload time series before X_{short}^{enc} and reflects the long term tendency in workload variation; X_{period} is the first period of workload for each machine; The y_{period} is the workload sequence corresponding to Y in the period of X_{period} . The extracting process of X_{period} and y_{period} is illustrated in section II-B1. We use $X_{long,i}^{enc}$ and $X_{short,i}^{enc}$ to denote the i -th time slot's workload in X_{long}^{enc} and X_{short}^{enc} respectively.

The three kinds of information (i.e. short-term dependent information, long-term tendency information and periodic information) bring different effects on workload prediction. The short-term dependent information X_{short}^{enc} is highly related to the predicting sequence, as the customers' behaviors are continuous and the workload is similar in a short time slot. The long-term tendency information denotes the forthcoming heavy load, as the heavy load is more likely to happen in ascending tendency. This tendency information is usually masked by noises in the short term and has to be extracted from long-term time series. As shown in Fig. 3(b), we pick a small segment of the workload from a long-term-ascending sequence. Though the long-term ascending tendency it is, the short-term workload just fluctuates around a stable value and does not show any increasing tendency. The periodic

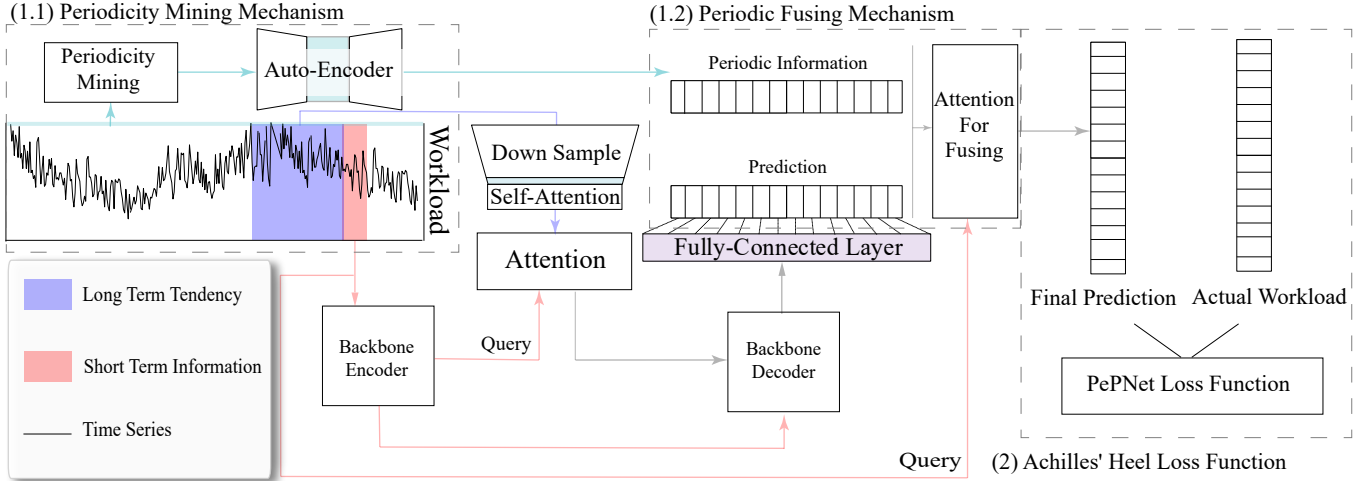


Fig. 2. The overview of PePNet.

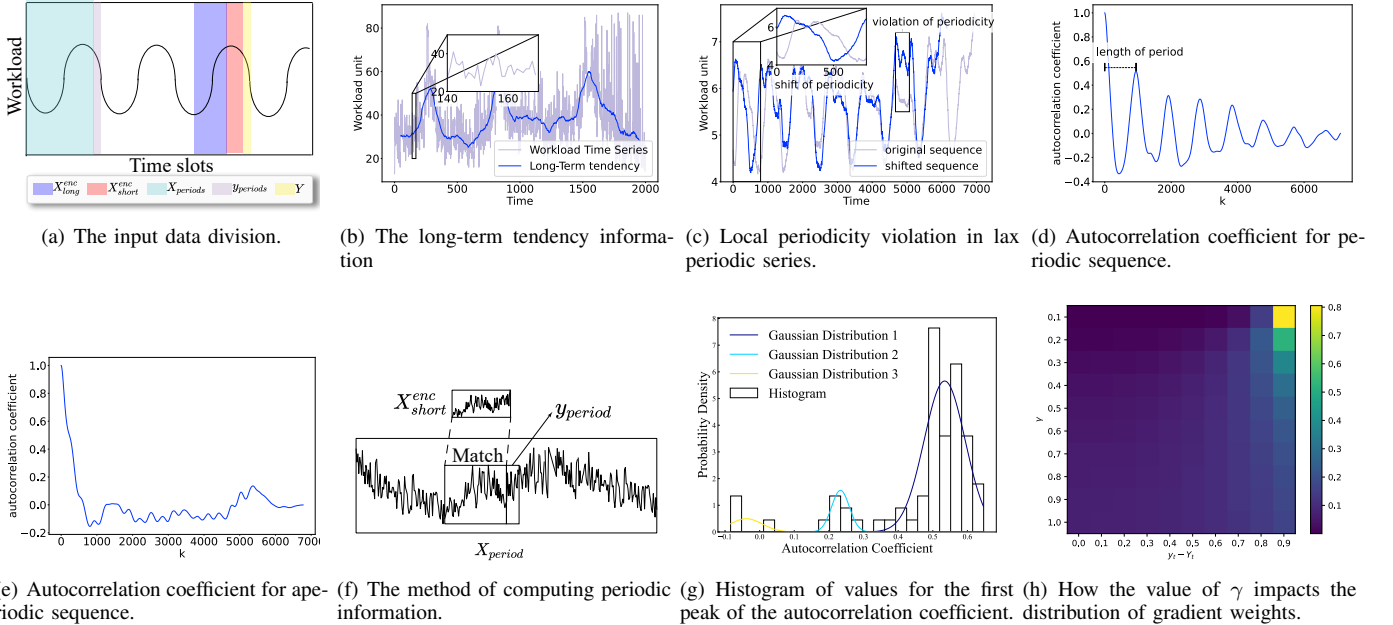


Fig. 3. Illustrations for data division and periodicity-perceived mechanism.

information provides the recurrent patterns in history and promotes both overall prediction accuracy and heavy-load prediction accuracy.

A. Overview of PePNet

PePNet is based on an encoder-decoder [18] architecture and fuses three kinds of information from rough data: the long-term tendency information, the short-term dependent information and the periodic information. Besides, the whole model is trained by an *Achilles' Heel Loss Function* to offset the negative impact of data imbalance. The overview of PePNet is shown in Fig. 2.

In the encoder, PePNet uses a backbone encoder, which can be implemented as many popular time-series-manipulating structures, such as transformer [19], LSTM [20] etc., to capture short-term dependent information from X_{short}^{enc} and uses

Periodicity-Mining Module to detect and extract periodic information from X_{period} . As for long-term tendency information, PePNet firstly downsamples X_{long}^{enc} , as it helps to improve the processing efficiency as well as maintain and magnify the trend information of time series. Then, PePNet uses self-attention to manipulate the down-sampled sequence. The processes of extracting short-term, long-term and periodic information are shown in Eq.1-3. In function $\text{Attention}(q, k, v)$, q, k, v respectively stand for the query, key and value [21].

$$\bar{X}_{short, i+1}^{enc} = \text{Backbone-Encoder}(X_{short, i}^{enc}) \quad (1)$$

$$y_{period}, X_{period} = \text{PeriodicityMining}(X, X_{short}^{enc}) \quad (2)$$

$$\bar{X}_{long}^{enc} = \text{Downsample}(\text{Attention}(X_{long}^{enc}, X_{long}^{enc}, X_{long}^{enc})) \quad (3)$$

In the decoder, PePNet uses a backbone-decoder, which can be implemented as many popular time-series-manipulating

structures, such as transformer, LSTM, etc., to generate $\hat{y} \in \mathbb{R}^{J \times d}$, where J stands for the predicting length. When using recurrent neural networks such as LSTM or GRU, the concatenation of h_j in Eq. 4 serves as the hidden state, and \hat{y}_j serves as the network input. When using a transformer or its variants, \hat{y}_j serves as the query and h_j serves as both the keys and values. After that, PePNet uses *Periodicity-Fusing Module* to estimate the reliability of \hat{y} and fuses it with y_{period} according to their reliability. By then, the *Periodicity-Fusing Module* generates the final prediction y . The process of decoder is shown in Eq.4-6, where W_h, W_c are both model parameters.

$$\hat{y}_{j+1} = \text{Backbone-Decoder}(\hat{y}_j, h) \quad (4)$$

$$h = \text{Attention}(X_{short}^{enc}, \bar{X}_{long}^{enc}, \bar{X}_{long}^{enc}) \quad (5)$$

$$y = \text{PeriodicityFusing}(X_{short}^{enc}, y_{period}, \hat{y}) \quad (6)$$

When training the model, the imbalance between heavy load and normal workload usually leads to unsatisfactory accuracy of heavy load prediction. Thus, we propose an *Achilles' Heel Loss function*, which aims to minimize the upper bound of prediction error. At each step, *Achilles' Heel Loss Function* iteratively optimizes the most under-fitting part for this step, in order to improve the prediction accuracy of the heavy load when keeping the overall prediction accurate. It is named after Achilles' Heel as it focuses on the most vulnerable portion along the predicting sequence. Thus, the prediction accuracy of the heavy load becomes more accurate, when keeping the overall prediction accurate.

B. Periodicity-Perceived Mechanism

Periodic information can effectively improve the overall prediction accuracy as well as the heavy workload prediction accuracy. It consists of *Periodicity-Mining Module* and *Periodicity-Fusing Module*.

There are three main challenges to fuse periodic information. (1) We have no priori knowledge about the periodicity of workload for different machines, which calls for the *Periodicity-Mining Module* to detect the existence of periodicity and the length of one period. (2) The periodicity for different machines is variable (i.e., strict periodic, lax periodic, aperiodic), which calls for an adaptive *Periodicity-Fusing Module*. (3) It is hard to fuse the periodic information in lax periodic series because lax periodic series are sometimes periodic and sometimes not. In Fig. 3(c), we overlap a series shifted one period ahead and the original series. As Fig. 3(c) shows, there are mainly two obstacles to fuse periodic information in lax periodic series: periodic shift and local periodicity violation. The former one can be solved by dynamic matching which is depicted in section *Periodicity-Mining Module*. The latter is caused by noise and external events. Therefore, we filter out the noise in periodic information in *Periodicity-Mining Module* and evaluate the reliability of periodic information in the *Periodicity-Fusing Module*.

1) *Periodicity-Mining Module*: PePNet calculates the time series autocorrelation coefficient ρ_k for each machine as shown in Eq.7, which represents the linear correlation among all workloads with interval k (i.e., linear correlation between X_t and X_{t-k} , for every $t \in \{t \in \mathbb{N}^+ | t < \text{sequence length}\}$, X_t stands for the workload at t -th time slot). As shown in Fig. 3(d), when the workload is periodic, the autocorrelation coefficient rises to a large value again after the first decline, which represents a high hop relevance of workload. While the sequence is aperiodic, the autocorrelation coefficients are shown in Fig. 3(e), which have a distinct pattern. Therefore, PePNet sets a hyperparameter \mathcal{T} and judges whether a time series is periodic by detecting whether the autocorrelation coefficient crosses over \mathcal{T} again. The value of \mathcal{T} denotes the acceptable range of periodicity strictness.

$$\rho_k = \frac{\text{cov}(X_{t-k}, X_t)}{\sqrt{\text{cov}(X_t, X_t)\text{cov}(X_{t-k}, X_{t-k})}} \quad (7)$$

The position of the first peak in autocorrelation coefficients of periodic sequence strikes the highest hop relevance and denotes the length of one period. We illustrate it in Fig. 3(d). The reason why the autocorrelation coefficient shows such a pattern is that the user behavior is continuous in time, so the autocorrelation coefficients of small k are large. As the time interval k increases, the relevance drops down. But when the time interval k reaches around the integer multiple of period length, the workload at the two moments X_t and X_{t-k} shows a high linear correlation again.

Based on these observations, as shown in Algorithm 1, PePNet traverses the value of k from small to large. If PePNet finds the smallest k that makes the autocorrelation coefficient ρ_k satisfy the conditions: $\rho_k > \rho_{k-1}, \rho_k > \rho_{k+1}$ and $\rho_k > \mathcal{T}$, the time series is periodic and the length of one period is k . Otherwise, the time series is aperiodic. We cut out the first period of the machines whose workloads are periodic in the training set as a periodic information knowledge base, which is denoted by X_{period} . To solve the issue of period shift, PePNet uses a dynamic matching. If the workload is periodic, PePNet finds the sequence $\{X_{t_a}, \dots, X_{t_a+I-1}\}$ in X_{period} , whose distance from X_{short}^{enc} is the smallest. The distance can be computed either by Mean Square Error (MSE) or by Dynamic Time Warping (DTW). Then, PePNet sets $y_{period} = \{X_{t_a+I}, \dots, X_{t_a+I+J}\}$. Otherwise, $\{-1, -1, \dots, -1\}$ is set to y_{period} . Such a process is illustrated in Fig. 3(f).

Error estimation. We use $E[(X_{t-k} - X_t)^2]$ to measure the quality of periodic length k found by the *Periodicity-Mining Module*. We have the following result, where $\sigma_{t-k}, \sigma_t, \mu_{t-k}, \mu_t$ are the standard deviation and expectation at $t-k$ and t time slots respectively. The $\Delta\sigma$ and $\Delta\mu$ are $\sigma_{t-k} - \sigma_t$ and $\mu_{t-k} - \mu_t$ respectively. σ is the standard deviation of a stationary time series.

Theorem 1. When using Algorithm 1, $E[(X_{t-k} - X_t)^2]$ is upper bounded by $(\Delta\sigma)^2 + (\Delta\mu)^2 + 2(1 - \mathcal{T})\sigma_{t-k}\sigma_t$. Furthermore, when the time series is stationary, $E[(X_{t-k} - X_t)^2]$ is upper bounded by $2(1 - \mathcal{T})\sigma^2$.

Proof of Theorem 1. According to algorithm 1, when PePNet finds k , Eq.8-9 holds, where $a_i = X_i - \mu_i, \hat{t} = t - k$. $E[(X_{\hat{t}} - X_t)^2]$ can be transformed to Eq.10. Then, we substitute Eq.9

Algorithm 1: Periodicity-Mining Module

Data: Workload time series X , Short-term dependent information X_{short}^{enc}
Result: The periodic information for prediction y_{period} , The periodic knowledge base X_{period}

```

1  $k \leftarrow -1$ ;
2 while  $k < \text{length}(X)$  do
3    $k \leftarrow k + 1$ ;
4   Compute  $\rho_k$ ;
5   if  $\rho_k > \rho_{k-1}$  and  $\rho_k > \rho_{k+1}$  and  $\rho_k > \mathcal{T}$  then
6     Period length= $k$  ;
7     FoundPeriodLength=True ;
8     break ;
9   end
10 end
11 if FoundPeriodLength then
12    $X_{period} = X[: \text{Period length}]$ ;
13    $y_{pos} = \arg \min_{t_a} \text{Distance}(X[t_a : t_a + I], X_{short}^{enc})$ ;
14    $y_{period} = X[y_{pos} : y_{pos} + I]$ ;
15 end
16 else
17    $X_{period} = -1$ ;
18    $y_{period} = [-1, \dots, -1]$ ;
19 end

```

into Eq.10 and obtain Eq.11. The Eq.11 can be further reduced into Eq.12 and the first part of Theorem 1 is proven. When the time series is stationary, $\Delta\sigma^2$ and $\Delta\mu^2$ are zero. Then the upper bound can be reduced to $2(1 - \mathcal{T})\sigma_{t-k}\sigma_t$.

$$\frac{E[a_{\bar{t}}a_t]}{\sigma_{\bar{t}}\sigma_t} > \mathcal{T} \quad (8)$$

$$E[a_{\bar{t}}a_t] > \mathcal{T} * \sigma_{\bar{t}}\sigma_t \quad (9)$$

$$E[(X_{\bar{t}} - X_t)^2] = E[a_{\bar{t}}^2 + a_t^2 - 2a_{\bar{t}}a_t + 2\Delta\mu\Delta a + \Delta\mu^2] \quad (10)$$

$$E[(X_{\bar{t}} - X_t)^2] < E[a_{\bar{t}}^2] + E[a_t^2] - 2 * \mathcal{T} \sqrt{E[a_{\bar{t}}^2]E[a_t^2]} + \Delta\mu^2 \quad (11)$$

$$E[(X_{\bar{t}} - X_t)^2] < \Delta\sigma^2 + \Delta\mu^2 + 2(1 - \mathcal{T})\sigma_{\bar{t}}\sigma_t \quad (12)$$

Taking a further look at the upper bound, the first and second items of the upper bound are constants. Thus, the value of error depends on the last item, which is determined by the value of \mathcal{T} . Considering that the \mathcal{T} is less than or equal to one, the closer the \mathcal{T} is to one, the smaller the error is. However, most of the time series are lax periodic in reality. Setting the \mathcal{T} as 1 may miss many lax periodic time series. Thus, there is a tradeoff between improving the accuracy of periodic length and finding all the periodic time series (including lax periodic time series).

Considering the tradeoff may make it challenging to choose a proper value of \mathcal{T} , we provide an automatic setting method for \mathcal{T} based on statistical observations. For finer tuning, this method provides a searching range for \mathcal{P} . The hyperparameter \mathcal{P} is a threshold setting for the first peak of the autocorrelation coefficient. Thus, we look into the distributions of the first peak

TABLE II
PARAMETERS OF GAUSSIAN DISTRIBUTION.

	weight	expectation	std
Gaussian distribution 1	0.84	0.53	0.06
Gaussian distribution 2	0.10	0.23	0.03
Gaussian distribution 3	0.06	-0.04	0.05

value. Taking Alibaba2018-CPU³ as an example, we take 75 machines in it and plot a histogram of first-peak value in Fig. 3(g). There are two properties of the distribution: clustered and following Gaussian Distribution for each cluster. We use the Gaussian Mixture Model (GMM) algorithm to fit the mixed Gaussian distribution of its first peak values and plot the Gaussian distributed curve on the histogram in Fig. 3(g). The parameter for this GMM is given in Tab. II, where "std" is the shorthand for standard deviation. Different clusters have different degrees of periodicity. The higher the expectation of the cluster is, the stricter its periodicity is. To guarantee the quality of the periodicity the *Periodicity-Mining Module* detects, it picks the workload in the cluster with the highest expected value as periodic and filters the others. Let μ and σ denote the expectation and standard deviation of the cluster with the highest expectation. In industrial applications, $\mu - \sigma$ can be directly used as the \mathcal{P} to save the labor costs, as the probability that the first peak is greater than $\mu - \sigma$ in this cluster is 84.2% according to Gaussian distribution. For finer tuning, the *mathcal{P}* can be explored between $\mu - \sigma$ and $\mu + \sigma$.

2) *Periodicity-Fusing Module*: To filter out the random noise in the periodic information, PePNet firstly uses an auto-encoder [22]. To solve the problem of variable periodicity for different machines and the problem of local periodicity violation, PePNet uses an attention mechanism to evaluate the reliability of periodic information. The final prediction y is given in Eq.13-14.

$$\hat{y}_{period} = \text{Autoencoder}(y_{period}) \quad (13)$$

$$y = \text{Attention}(X_{short}^{enc}, (\hat{y}, \hat{y}_{period}), (\hat{y}, \hat{y}_{period})) \quad (14)$$

C. Achilles' Heel Loss Function

Heavy load rarely occurs, which leads to poor performance of heavy load prediction due to data imbalance. To solve this problem, PePNet deploys the Achilles' Heel Loss Function. As analyzed below, the Achilles' Heel Loss Function actually forces the loss to descend along the gradient directions of some of the largest prediction errors. When iteratively training the model, the Achilles' Heel Loss Function optimizes the most under-fitting part in one step. In the next step, the original largest prediction error diminishes and the most under-fitting part shifts to another place. In this way, the Achilles' Heel Loss Function optimizes each part of the sequence iteratively and effectively improves the accuracy of heavy load, when keeping high predicting accuracy of overall workload. The Achilles' Heel Loss Function is given in Eq.15, where T equals $\{t_1, \dots, t_{1+J}\}$, which are the time slots of a forecasting

³<https://github.com/alibaba/clusterdata>

sequence. y_t denotes the predicted workload at time t (the prediction length for one sample should be at least 2), Y_t denotes the ground-truth workload at time t , and γ is a hyperparameter.

$$l(Y, y) = \gamma \log\left(\sum_{t \in T} \exp\left(\frac{(y_t - Y_t)^2}{\gamma}\right)\right), \gamma > 0 \quad (15)$$

The Achilles' Heel Loss Function actually distributes more weight to the gradient for higher prediction error when back propagating. This aspect is obvious by deriving Eq.15, as shown in Eq.16, where $\alpha_t = \frac{\exp(\frac{(y_t(\mathcal{P}) - Y_t)^2}{\gamma})}{\sum_{t=1}^T \exp(\frac{(y_t(\mathcal{P}) - Y_t)^2}{\gamma})}$, \mathcal{P} stands for the parameters of PePNet. α_t is actually a normalized weight, whose value depends on the prediction error at time slot t . γ is a scale factor. When γ is large, the difference in prediction errors across time slots is narrowed and the weights are relatively uniform for each time slot. When the γ is small, the difference in prediction errors across time slots is amplified and the weights become polarized. To visually demonstrate this point, we plot the value of α_t for different combinations of γ and prediction error $y_t - Y_t$ in Fig. 3(h). In Fig. 3(h), each row shows the value of α_t for a set of prediction error $\{y_t - Y_t | 0 \leq t \leq 9\}$, when specifying the γ . As Fig. 3(h) shown, for a specific γ , the larger the prediction error is, the bigger the α_t is. Besides, for a specific prediction error in a specific error set, the smaller the γ is, the bigger the α_t is. When γ is set to 0.1, α_t for the largest prediction error in this row approximates 1.

$$\frac{\partial l(Y, y)}{\partial \mathcal{P}} = \sum_{t=1}^T (\alpha_t \cdot \frac{\partial (y_t(\mathcal{P}) - Y_t)^2}{\partial \mathcal{P}}) \quad (16)$$

It is worth noticing that when the γ is indefinitely close to 0, the Achilles' Heel Loss Function becomes a simple formation, which is given in the following theorem. The theorem implies that when γ indefinitely approximates 0, only the gradient for maximum prediction error is assigned a weight of 1, while others are assigned a weight of 0.

Theorem 2. As the γ is infinitely close to 0, the gradient of the loss function infinitely approximates Eq.17. The $t^* = \arg \max_t (y_t - Y_t)^2$ and the $g(t^*, \mathcal{P}) = (y[t^*] - Y[t^*])^2$.

$$\frac{\partial l(Y, y)}{\partial \mathcal{P}} = \frac{\partial g(t^*, \mathcal{P})}{\partial \mathcal{P}} \quad (17)$$

Proof of Theorem 2. The derivation of $l(Y, y)$ is shown in Eq.18. Then, both the numerator and dominator on the right-hand side are divided by $\exp(\frac{g(t^*, \mathcal{P})}{\gamma})$ simultaneously and the first step of Eq.19 is obtained. The $g(t^*, \mathcal{P})$ is surely bigger than $g(t, \mathcal{P}), \forall t \neq t^*$, as the definition of t^* suggests. Thus, $g(t, \mathcal{P}) - g(t^*, \mathcal{P}) < 0, \forall t \neq t^*$. When the $\gamma (\gamma > 0)$ infinitely approaches zero, $\exp(\frac{g(t, \mathcal{P}) - g(t^*, \mathcal{P})}{\gamma})$ will also infinitely approaches zero. In this way, the second step of Eq.19 is obtained.

$$\frac{\partial l(Y, y)}{\partial \mathcal{P}} = \frac{\sum_t^T [\exp(\frac{g(t, \mathcal{P})}{\gamma}) \frac{\partial g(t, \mathcal{P})}{\partial \mathcal{P}}]}{\sum_t^T \exp(\frac{g(t, \mathcal{P})}{\gamma})} \quad (18)$$

$$\begin{aligned} & \lim_{\gamma \rightarrow 0} \frac{\partial l(Y, y)}{\partial \mathcal{P}} \\ &= \lim_{\gamma \rightarrow 0} \frac{\frac{\partial g(t^*, \mathcal{P})}{\partial \mathcal{P}} + \sum_{t, t \neq t^*}^T [\exp(\frac{g(t, \mathcal{P}) - g(t^*, \mathcal{P})}{\gamma}) \frac{\partial g(t, \mathcal{P})}{\partial \mathcal{P}}]}{1 + \sum_{t, t \neq t^*}^T \exp(\frac{g(t, \mathcal{P}) - g(t^*, \mathcal{P})}{\gamma})} \\ &= \frac{\partial g(t^*, \mathcal{P})}{\partial \mathcal{P}} \end{aligned} \quad (19)$$

III. EXPERIMENT

In this section, we conduct extensive experiments to validate the following findings:

- PePNet improves the accuracy of heavy-workload prediction as well as the overall prediction accuracy compared with the state-of-the-art methods.
- PePNet only introduces slight time overhead for training and inference.
- PePNet is insensitive to hyperparameters and has high robustness.
- Each mechanism in PePNet is proven to play an important role by using ablation experiments.
- Due to its adaptability for periodicity, when the time series is aperiodic, PePNet still works well.

TABLE III
BASIC HYPERPARAMETERS OF PEPNET.

Hyperparameter	Value
Batchsize of Alibaba2018-CPU	100
Learning rate of Alibaba2018	0.001
Learnig rate of Dinda's dataset	0.0005
Learning rate of SMD	0.01
\mathcal{T} of Alibaba2018-Mem	0.2
\mathcal{T} of others	0.5
γ	$\lim_{\gamma \rightarrow 0}$
Number of layers of LSTM	2
Input length of Alibaba2018 for short-term information	50
Input length of Alibaba2018 for long-term information	100
Input length of Dinda's dataset for short-term information	30
Input length of Dinda's dataset for long-term information	80
Input length of SMD for short-term information	50
Input length of SMD for long-term information	100
Hidden layer size of LSTM	80
Predicted length	2
Init downsampling step size	20
Number of layers of auto-encoder	1
Number of layers of auto-decoder	1
Output size of auto-encoder	1
Sliding window length for downsampling	100

A. Experiment Setup

Hyperparameters. We summarize the most important hyperparameters of PePNet in Tab. III.

Baseline Methods. We compare PePNet with the state-of-the-art time series predicting methods and popular workload predicting models and the variants of PePNet.

- **Autoformer (Autof) [23]:** Autoformer is a novel decomposition architecture with an Auto-Correlation mechanism. It breaks the pre-processing convention of series decomposition and renovates it as a basic inner block of deep models. Further, Autoformer also has an Auto-Correlation mechanism based on the series periodicity.
- **LSTM with attention mechanism (LSTMa) [10]:** The approach extracts the sequential and contextual features

of the historical workload data by an encoder network and integrates an attention mechanism into the decoder network.

- **Informer (Inf) [11]:** The method uses a *ProbSparse* attention mechanism and a halving cascading layer to extract the input information and use a generative style decoder to predict. Informer is one of the most recognized methods of time series prediction in recent years.
- **L-PAW [5]:** The method integrates top-sparse auto-encoder (TSA) and gated recurrent unit (GRU) block into RNN to achieve the adaptive and accurate prediction for highly-variable workloads. L-PAW is a model specifically designed for workload prediction and is also widely used.
- **LSTM [20]:** A classic time series processing model, which uses the hidden state to store long sequences of information.
- **GRU [18]:** A variant of the LSTM that modifies the forget gate structure in LSTM to make the model simpler.
- **Reformer (Ref) [24]:** Reformer introduces two techniques to improve the efficiency of Transformers. Firstly, it replaces dot-product attention with one that uses locality-sensitive hashing. Secondly, it uses reversible residual layers instead of standard residuals to reduce the memory consumption of the model. It is a widely recognized method in time series prediction.
- **Fedformer (Fedf) [25]:** Fedformer combines Transformer with a seasonal-trend decomposition method, in which the decomposition method captures the global profile of time series while Transformers capture more detailed structures. Fedformer is an effective and novel method in time series prediction.
- **Variants of PePNet:** We implement the backbone-encoder and backbone-decoder as transformer and LSTM respectively and denote them as PePNet-I and PePNet-II. Without specification, we use PePNet to denote PePNet-II in the following. Moreover, we also introduce some variants for ablation study. We use PePNet⁻ to denote PePNet-II that removes the Periodicity-Perceived Mechanism. We use PePNet[†] to denote the PePNet-II that uses MSE as a loss function. We use PePNet[‡] to denote the PePNet-II that both removes the Periodicity-Perceived Mechanism and does not use the Achilles' Heel loss function.

Datasets. We perform experiments on three public datasets: Alibaba's cluster trace v2018⁴, Dinda's dataset [12] and Server Machine Dataset (SMD) [26]. These datasets are collected by different organizations with different system configurations. Their use can help to verify the generalization of PePNet. We plot the data distribution of different datasets in Fig. 4(a). It is worth noting that different datasets represent different data distributions: long-tailed distribution (Dinda's dataset), centralized distribution (memory usage of Alibaba2018 and SMD), and relatively even data distribution (CPU usage of Alibaba2018).

- **Dinda's dataset (long-tailed distribution):** Dinda's dataset is collected from two groups of machines. The

first is the Alpha cluster at the Pittsburgh Supercomputing Center (PSC). The second one includes computing servers (Mojave, Sahara), a testbed (manchester1-8), and desktop workstations at Carnegie Mellon University. The workload in Dinda's dataset shows significant periodicity and sometimes there are large peaks far above average (long-tailed distribution).

- **Alibaba2018-Memory (centralized distribution):** Alibaba's cluster trace is sampled from one of Alibaba's production clusters, which includes about 4000 machines' workload in 8 days. Memory usage of some machines in this dataset shows relatively significant periodicity and others are aperiodic. Memory usage is generally stable and is distributed around a certain value (centralized distribution).
- **Alibaba2018-CPU (relatively even distribution):** The CPU usage in Alibaba2018 shows more significant periodicity on the heavy workload than the light load. Besides, it is highly variable and is distributed relatively even.
- **SMD dataset (centralized distribution with rare extreme values):** SMD is a new 5-week-long dataset, which is collected from a top 10 Internet company. SMD is made up of data from 28 different machines. It consists of 38 features, including CPU utilization, memory utilization, disk I/O, etc. The workload in this dataset shows high periodicity. Besides, most of the workload of this dataset is concentrated around 10-20, while others are extremely big.

We use the first 1,000,000 lines in Alibaba's dataset and *axp0* in Dinda's dataset. The values in Alibaba2018 are utilization percentage and we uniformly scale it to range [0, 1].

Evaluation metrics. We use three metrics to evaluate PePNet's performance: Mean Squared Error (MSE), Mean Absolute Error (MAE), and Mean Absolute Percentage Error (MAPE). These metrics are some of the most recognized and widely used ones in time series prediction. There are many influential works using these metrics, such as [11], [5], [23]. Besides, these metrics not only measure the relative error (MAPE) but also the absolute error (MSE, MAE).

B. Prediction Accuracy

We summarize the performance of all the methods in Tab. IV. We use the above metrics to evaluate the accuracy of heavy-workload forecasting accuracy as well as overall forecasting accuracy. We highlight the highest accuracy in boldface. Besides, if PePNet achieves the highest accuracy, we highlight the best one in baseline with underlines.

As shown in Tab. IV, PePNet achieves the best heavy-workload prediction accuracy as well as overall prediction accuracy on all three workload datasets, with few exceptions. Comparing the prediction accuracy on all three datasets, PePNet works the best on long-tail distributed Dinda's dataset, while less advantageous on the relatively even-distributed Alibaba2018-CPU dataset.

Long-tail data distribution. PePNet works best in this case. Compared with the best performance among the baselines,

⁴<https://github.com/alibaba/clusterdata>

TABLE IV

THE OVERALL AND HEAVY-WORKLOAD PREDICTION ACCURACY ON THREE DATASETS. THE MSE IN THE TABLE ARE MULTIPLIED BY 1000.

			LSTM	LSTMa	GRU	Inf	L-PAW	Ref	Autof	Fedf	PePNet ⁻	PePNet [†]	PePNet [‡]	PePNet-I	PePNet-II
Dinda's Dataset	Overall	MAPE	<u>0.093</u>	0.117	0.108	0.100	0.102	0.104	0.211	0.110	0.089	0.087	0.116	0.047	0.076
		MSE	5.515	8.233	9.516	<u>4.865</u>	10.960	8.950	37.636	9.211	5.773	6.146	6.847	4.420	3.697
		MAE	0.048	0.071	0.070	<u>0.041</u>	0.078	0.053	0.149	0.057	0.046	0.049	0.059	0.054	0.029
	Heavy-Workload	MAPE	0.051	0.079	0.094	<u>0.030</u>	0.046	0.040	0.079	0.032	0.035	0.043	0.058	0.065	0.018
		MSE	12.260	17.925	24.191	<u>6.837</u>	15.853	9.202	23.817	8.729	5.635	7.325	13.274	8.760	6.124
		MAE	0.068	0.104	0.123	<u>0.040</u>	0.058	0.051	0.097	0.041	0.046	0.057	0.076	0.083	0.025
SMD Dataset	Overall	MAPE	<u>0.179</u>	0.238	0.287	0.237	0.296	0.278	0.488	0.290	0.207	0.191	0.161	0.076	0.154
		MSE	3.434	3.627	3.889	3.282	3.909	4.950	8.021	<u>2.350</u>	3.144	2.974	3.101	0.552	1.757
		MAE	<u>0.019</u>	0.023	0.025	0.022	0.025	0.028	0.046	0.023	0.020	0.019	0.018	0.015	0.014
	Heavy-Workload	MAPE	<u>0.150</u>	0.163	0.154	0.166	0.154	0.316	0.367	0.157	0.138	0.129	0.158	0.204	0.112
		MSE	10.437	10.622	11.945	11.024	11.912	17.587	27.465	<u>5.531</u>	10.941	9.751	10.399	4.138	6.729
		MAE	0.037	0.045	0.046	0.041	0.046	0.068	0.095	<u>0.034</u>	0.042	0.038	0.040	0.055	0.033
Alibaba Memory	Overall	MAPE	0.039	0.095	0.049	0.058	<u>0.157</u>	0.086	0.037	0.025	0.050	0.027	0.126	0.017	0.016
		MSE	<u>0.375</u>	0.489	0.462	0.408	12.721	0.880	1.173	0.510	0.359	0.341	0.975	0.410	0.323
		MAE	<u>0.014</u>	0.017	0.015	0.015	0.058	0.023	0.026	0.016	0.014	0.013	0.024	0.014	0.013
	Heavy-Workload	MAPE	0.023	0.023	0.027	0.027	0.039	<u>0.022</u>	0.032	0.030	0.019	0.019	0.030	0.019	0.019
		MSE	0.706	<u>0.673</u>	0.860	0.919	2.420	0.695	1.418	1.182	0.566	0.542	1.114	0.598	0.509
		MAE	0.021	0.020	0.023	0.024	0.032	<u>0.019</u>	0.029	0.027	0.018	0.018	0.028	0.018	0.017
Alibaba CPU	Overall	MAPE	0.173	0.215	0.181	0.165	0.272	0.190	0.258	<u>0.158</u>	0.139	0.158	0.150	0.153	0.142
		MSE	4.647	4.996	4.753	4.809	12.638	6.097	9.954	6.204	4.786	4.812	4.784	6.039	4.758
		MAE	0.049	0.053	0.051	0.050	0.090	0.060	0.073	0.056	0.050	0.051	0.050	0.054	0.049
	Heavy-Workload	MAPE	0.195	0.237	0.194	<u>0.193</u>	0.343	0.247	0.381	0.252	0.178	0.177	0.182	0.176	0.143
		MSE	16.767	17.548	<u>16.228</u>	17.742	29.493	18.848	32.271	22.226	16.594	16.321	16.405	14.090	11.634
		MAE	<u>0.095</u>	0.100	0.096	0.100	0.150	0.105	0.145	0.115	0.097	0.095	0.095	0.087	0.082

PePNet improves MAPE, MSE, and MAE by 17.9%, 24.0%, and 29.5% respectively for overall prediction. For heavy-workload prediction, PePNet improves MAPE, MSE, and MAE by 40.8%, 10.4%, and 38.7% respectively over the best method in the baseline.

Centralized data distribution with rare extreme value. PePNet also has obvious advantages in this case, because the SMD dataset has extremely heavy workload. Compared with the best performance in the baseline, PePNet improves MAPE, MSE and MAE by 14.0%, 25.2% and 26.7% respectively for overall prediction. For heavy-workload prediction, PePNet improves MAPE and MAE by 25.3% and 25.0% respectively.

Centralized data distribution. PePNet is also effective in this case. Compared with the best performance in the baseline, PePNet improves MAPE, MSE and MAE by 33.8%, 13.9% and 9.5% for overall prediction. For heavy-workload prediction, PePNet improves MAPE, MSE and MAE by 15.2%, 24.4% and 8.7% respectively, compared with the best method in the baseline.

Relatively even data distribution. In this case, PePNet maintains high overall prediction accuracy and achieves the best heavy workload prediction performance among neural network-based methods. PePNet improves MAPE, MSE and MAE by 25.7%, 28.3% and 13.9% for heavy-workload prediction over the best method in the baseline.

C. Time Overhead

We use an Intel(R) Xeon(R) CPU E5-2620 @ 2.10GHz CPU and a K80 GPU to record the time spent on training and inference for all methods. We show the time overhead of all the methods in Fig. 4(b). PePNet brings just an acceptable extra time overhead compared to the most efficient network (GRU) and greatly improves the overall and heavy-workload

prediction accuracy, especially on Dinda's dataset (40.8% for MAPE of heavy-workload prediction).

D. Hyperparameter Sensitivity

The impact of input length and prediction length. We use grid search to explore the impact of X_{short}^{enc} 's length and the impact of y 's length on PePNet's performance. We show the result in Fig. 4(d)-Fig. 4(i). We perform experiments with Cartesian combinations of input lengths from 30 to 80 and prediction lengths from 2 to 12. Generally, the error grows higher gently when predicting length increases. The best input length for different datasets is different. It is found the best input length for Alibaba2018-Memory and Alibaba2018-CPU is 50, while the best input length for Dinda's dataset is 30.

Dinda's dataset. For overall workload prediction, MAE rises slowly as prediction length increases and MAE is stable for any input length. For heavy-workload workload prediction, MAE is more stable for prediction length when the input length is longer. As the length of prediction grows, the MAE for overall accuracy increases no more than 0.051 at each input length, while the MAE of heavy workload increases no more than 0.062.

Alibaba2018-Memory. The long-term dependency of Alibaba's memory usage is weak, thus when the input length is too big, increasing the input length increases the noise level, which could corrupt the performance of PePNet. Thus, when the input length is greater than 50, the MAE of PePNet is unstable. But when the input length is less than 50, the performance of PePNet is stable, and the prediction error only increases slowly with the prediction length. For overall memory usage prediction, the MAE with a prediction length of 12 is only 0.006 larger than the MAE with a prediction length of 2. For heavy-workload memory usage prediction, the MAE

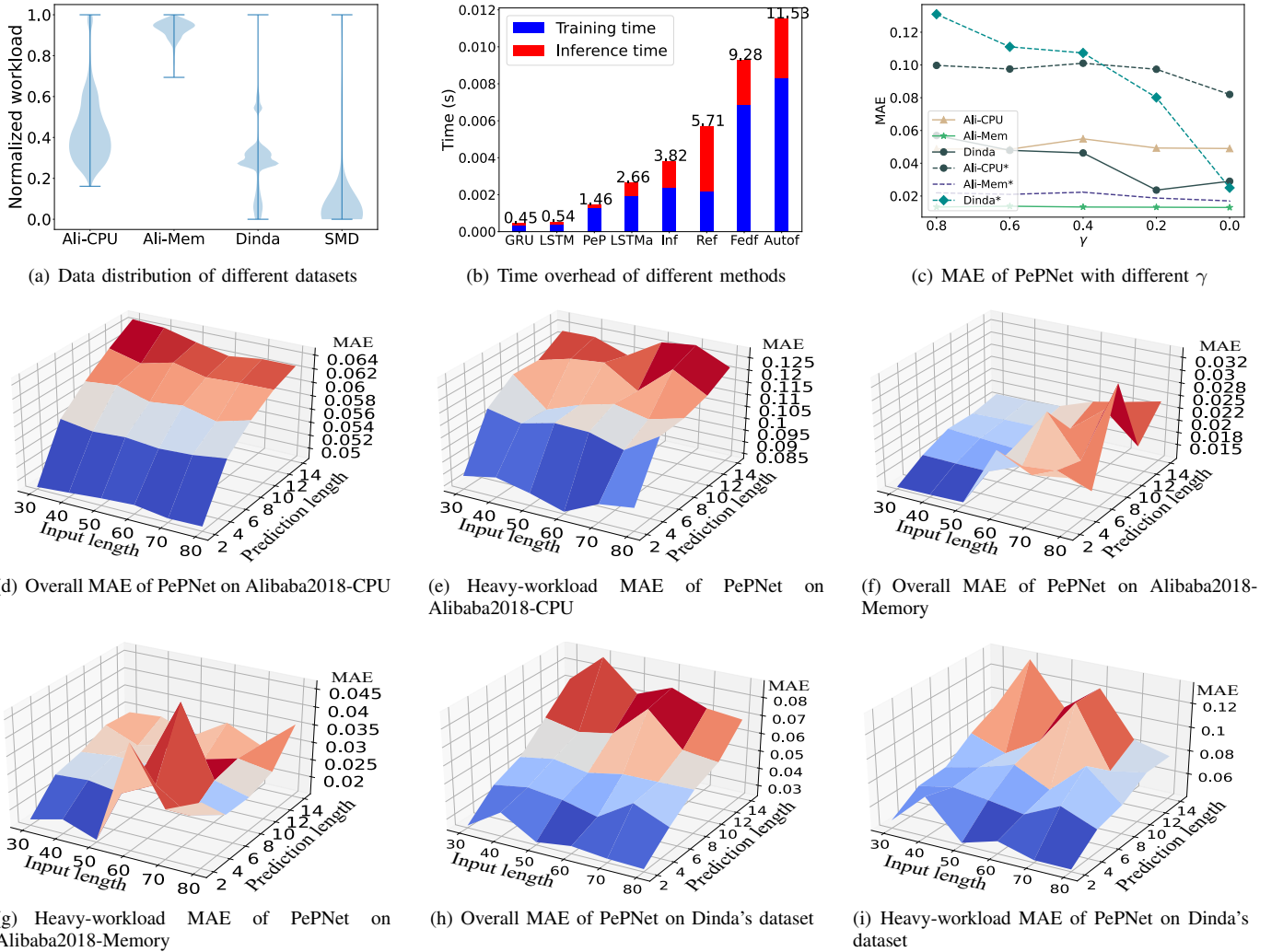


Fig. 4. (a) The value of the y-axis is the original workload divided by the maximum workload of its machine. The wider the width of the violin in the figure is, the more workloads are distributed near this value. (b) The figure shows the average consuming time of one forward propagation and backpropagation for one sample. The labels on the histogram are 1000 times of the actual value. Besides, we use the shorthand of Informer, Autoformer and Reformer in the xticks. (c) The figure shows the overall and heavy-workload MAE of PePNet for different γ on all the three datasets. In the legend, we use dataset name* to represent the heavy-workload MAE on the specific dataset, while using dataset name to represent the overall MAE on the dataset. (d)-(i) These figures show overall and heavy-workload MAE of PePNet on different datasets with different combination of the length of X_{in} and p .

with a prediction length of 12 is only 0.012 larger than that with a prediction length of 2.

Alibaba2018-CPU. Long-term dependency is more pronounced in CPU usage. Thus, when we increase the input length, the performance of PePNet is always stable. For overall CPU usage prediction, the MAE with a prediction length of 12 is only 0.016 larger than that with a prediction length of 2. For heavy-workload CPU usage prediction, the MAE with a prediction length of 12 is only 0.034 larger than that with a prediction length of 2.

The impact of γ . We also explore the impact of γ on three datasets, as shown in Fig. 4(c). There are slight fluctuations of overall accuracy for different γ . Besides, it is consistent with the theoretical analysis in Section.II-C that when the γ is smaller the heavy-workload accuracy is higher. It is also intuitive that the heavy-workload MAE of Dinda's dataset dips most sharply, as Dinda's dataset is long-tail distributed. The extremely heavy workload in the long tail greatly reduces the prediction accuracy. But as γ gets smaller, more attention

is put on heavy workload, during the process of training. According to our experimental results, setting γ as the value indefinitely approaching zero can lead to the best accuracy. As analyzed in Section.II-C, when γ indefinitely approaches zero, Achilles' loss function only optimizes the part with the highest prediction error. In this situation, PePNet also achieves high prediction accuracy without overall accuracy degradation, which verifies that the Achilles' loss function helps to avoid overly emphasizing sporadic patterns.

E. Ablation Experiment

We validate the effect of the Periodicity-Perceived Mechanism and heavy-workload-focused loss function by comparing the performance of PePNet with that of PePNet⁻ and PePNet[†]. We show the performance of these models in Tab. IV and summarize the improvement ratio of PePNet compared with PePNet⁻ and PePNet[†] in Tab. V and Tab. VI respectively. Overall, the Periodicity-Perceived Mechanism contributes more to the prediction accuracy than the Achilles'

Heel loss function. But Achilles' Heel loss function can improve the accuracy of periodic and aperiodic time series, while the Periodicity-Perceived Mechanism can only promote the accuracy of periodic and lax-periodic data. Furthermore, we also test the prediction accuracy of PePNet on aperiodic data.

The performance of Periodicity-Perceived Mechanism.

Dinda's dataset and SMD dataset exhibit stricter periodicity than Alibaba2018 does [10]. Thus, the Periodicity-Perceived Mechanism promotes the prediction accuracy most on Dinda's dataset and SMD dataset. For datasets with lax periodicities, such as memory usage of Alibaba2018, the Periodicity-Perceived Mechanism also promotes overall and heavy-workload prediction accuracy. As for CPU usage of Alibaba2018, which has no significant periodicity on light load but has more significant periodicity on heavy workload, the Periodicity-Perceived Mechanism can promote the heavy-workload prediction accuracy, while the performance of PePNet is about as same as PePNet⁻ on light load. This observation confirms that the Periodicity-Perceived Mechanism has little negative impact on aperiodic data.

TABLE V
IMPROVEMENT (%) OF PEPNET OVER PEPNET⁻.

	Overall			Heavy-workload		
	MAPE	MSE	MAE	MAPE	MSE	MAE
Dinda's dataset	14.8	36.0	37.1	49.9	-8.7	46.6
SMD dataset	25.7	44.1	30.8	18.7	38.5	21.6
Alibaba2018-Memory	67.6	10.0	9.07	2.53	10.1	2.69
Alibaba2018-CPU	-2.1	0.60	0.30	19.4	29.9	15.1
Max.	67.6	44.1	37.1	49.9	38.5	46.6
Min.	-2.1	0.59	0.29	2.53	-8.7	2.69
Avg.	26.6	22.7	19.3	22.6	17.5	21.5

The performance of Achilles' Heel loss function. Our loss function can improve both the overall prediction accuracy and heavy-workload prediction accuracy on all three datasets, compared with PePNet[†]. Except MAPE for heavy-workload prediction accuracy on memory usage of Alibaba2018, all of the evaluation metrics of PePNet are better than that of PePNet[†]. As the Achilles' Heel Loss function apparently reduces the error for extremely heavy workload in the long tail, which is also proven in Fig. 4(c), the Achilles' Heel Loss Function improves the accuracy of Dinda's dataset and SMD dataset more than that of Alibaba2018.

TABLE VI
IMPROVEMENT (%) OF PEPNET OVER PEPNET[†].

	Overall			Heavy-workload		
	MAPE	MSE	MAE	MAPE	MSE	MAE
Dinda's dataset	12.2	39.8	40.4	59.4	16.4	56.6
SMD dataset	19.1	40.9	26.3	12.6	31.0	13.2
Alibaba2018-Memory	39.9	5.28	4.96	-1.3	6.09	0.66
Alibaba2018-CPU	10.3	1.10	2.10	18.9	28.7	13.6
Max.	39.9	40.9	40.4	59.4	31.0	56.6
Min.	10.3	1.12	2.13	-1.3	6.09	0.66
Avg.	20.4	21.8	18.5	22.4	20.6	21.0

The performance of PePNet on aperiodic data. There is a major concern about whether PePNet still works well on aperiodic data. To test the prediction accuracy on aperiodic data, we divide the Alibaba2018-CPU and Alibaba2018-Memory by periodicity and collect the prediction accuracy for periodic data and aperiodic data respectively. In Tab. VII, there is prediction accuracy for periodic data and aperiodic data.

TABLE VII
COMPARE THE PERFORMANCE OF PEPNET ON APERIODIC AND PERIODIC DATA. THE MSE ARE MULTIPLIED BY 1000. THE MAE ARE MULTIPLIED BY 100.

	Periodicity	Overall Metric			Heavy-workload		
		MAPE	MSE	MAE	MAPE	MSE	MAE
Ali2018-Memory	Periodic	0.024	0.08	0.47	0.018	0.17	0.95
	Aperiodic	0.015	0.35	1.35	0.019	0.53	1.78
	Both	0.016	0.32	1.27	0.019	0.51	1.74
Ali2018-CPU	Periodic	0.133	2.81	3.79	0.117	5.44	5.16
	Aperiodic	0.166	8.01	6.87	0.163	16.1	10.2
	Both	0.142	4.76	4.94	0.143	12.4	8.21

For convenience, the overall accuracy of both periodic data and aperiodic data is also listed at the bottom. On the whole, the accuracy of periodic data is slightly higher than the overall accuracy, while the accuracy of aperiodic data is slightly lower than the overall. However, there is a strange phenomenon the MAPE of periodic data in Alibaba2018-Memory is bigger than the overall accuracy, while its MAE and MSE are much lower than the overall accuracy. That is because, in the Alibaba2018-Memory dataset, the periodic workload is much smaller than the aperiodic one. Thus, even slight errors in periodic data prediction tend to become much larger after the division in the computation of MAPE.

IV. RELATED WORK

We first review existing methods for workload and time series prediction. Since PePNet uses periodic information, we also summarize related work for this topic.

A. Workload and Time Series Prediction

Time series prediction aims to predict future time series based on the observed workload data, while workload prediction aims to predict future workload based on observed ones. Present research predicts many different workloads, such as the GPU workload [27], CPU utilization [28], virtual desktop infrastructure pool workload [29], disk states [30], database query arrival rates [31] and so on. Researchers make workload predictions for different aims, such as cloud resource allocation [32], autoscaling [28], etc. Additionally, some works proposed an integrated framework of prediction models and other functional modules. For example, Uncertainty-Aware Heuristic Search (UAHS) [33] combines workload prediction models and Bayesian optimization to model the uncertainty and guide virtual machines (VMs) provision strategy. SimpleTS [34] deploys a framework that automatically selects a proper prediction model for a specific time series. However, these methods only focus on improving overall accuracy while neglecting high load accuracy.

As workload prediction is a branch of time series prediction, it is necessary to review the development of time series prediction. In this domain, several frequently discussed issues garner significant attention. One stream is to improve the prediction accuracy of dynamic real-world time series, especially the accuracy of long input sequences. The solutions for this problem can be roughly divided into four categories: the statistic-based methods [7] [35] [36], the recurrent neural networks [37] [38] [39], the transformer-based methods [23]

[24] [11] and the integrated methods [10] [40] [5]. The statistic-based methods are efficient but not robust for highly dynamic real-world time series. The recurrent neural networks improve this aspect but suffer from catastrophic forgetting effects. To conquer this drawback, the integrated methods combine attention mechanism [10] and auto-encoder [14] into the recurrent neural network. Transformer-based methods make further progress by utilizing transformers. Another time series prediction issue that receives widespread attention is the spatiotemporal forecasting problem. In this field, researchers improve the prediction accuracy by leveraging the spatial and temporal information with GNN, CNN, plugin modules and other neural networks [15] [41] [42] [43]. But these methods manually define the spatio-temporal blocks which capture the temporal and spatial correlations. To overcome this limitation, AutoCTS [44] automatically selects competitive heterogeneous spatiotemporal blocks. But these methods also ignore the under-fitting problem of extreme values. Another research direction is improving the robustness of deep networks dealing with time series. The robustness includes five implications: the robustness for missing data, the robustness for the malicious or limited labels, the generalization of the trained model, the robustness toward noise in time series, and the robustness for the irregular data sampling period. For example, Belkhouja et al. propose a Robust Training for Time-Series (ROTS) to improve deep neural network robustness for generalization and noise [45]; Tan et al. propose Dual-Attention Time-Aware Gated Recurrent Unit (DATA-GRU) to manipulate time series sampled in an irregular period [46]; Zhang et al. propose Multivariate Time Series Classification with Attentional Prototypical Network (TapNet) to deal with time series with limited labels [47]; Tang et al. propose network modeling local and global temporal dynamics (LGnet) to deal with a data-missing problem in time series [48]; Luo et al. propose E^2GAN , which uses adversarial learning to deal with data missing problem [49]; Yao et al. propose Spatial-Temporal Dynamic Network (STDN) to deal with lax-strict periodicity caused by noise [16]; Luo et al. propose Uncertainty-Aware Heuristic Search (UAHS) to deal with uncertain prediction error caused by noise [33]. However, none of these methods focus on dealing with the prediction accuracy of heavy workload.

B. Periodicity Information Extraction

In the field of traffic forecasting, there is also significant periodicity and we summarize some recent popular methods below. There are several mechanisms to fuse periodic information. For example, Guo et al. propose a novel attention-based spatial-temporal graph convolution network [13]; Lv et al. use a fully connected layer and take advantage of both CNN and RNN to deal with periodic time series [15]; Chen et al. propose Hop Res-RGNN to deal with periodic patterns [14]. However, these methods do not consider the lax periodicity of time series. Yao et al. propose an attention mechanism to tackle periodic shift [16]. These studies use the priori knowledge of the daily and weekly periodicity of traffic loads. However, in the scenario of service load prediction, there is usually no priori knowledge about the periodicity. Besides, the

periodicity of the time series in these studies is fixed, while the periodicities of workload for different machines are variable.

V. CONCLUSION

In this paper, we study the problem of improving overall workload prediction accuracy as well as heavy-workload prediction accuracy and propose PePNet. PePNet makes use of short-term dependent information, long-term tendency information and periodic information. Within PePNet, we propose two mechanisms for better prediction accuracy of workloads: (1) a Periodicity-Perceived Mechanism to guide heavy-workload prediction, which can mine the periodic information and adaptively fuse periodic information for periodic, lax periodic and aperiodic time series; and (2) an Achilles' Heel Loss Function to offset the negative effect of data imbalance. We also provide theoretical support for the above design by: (1) providing a theoretically proven error bound of periodic information extracted by *Periodicity-Perceived Mechanism*; and (2) providing an automatic hyperparameter determination method for periodicity threshold \mathcal{T} . Compared with existing methods, extensive experiments conducted on Alibaba2018, Dinda's dataset and SMD dataset demonstrate that PePNet improves MSE for overall workload prediction by 11.8% on average. Especially, PePNet improves MSE for heavy workload prediction by 21.0% on average.

ACKNOWLEDGMENTS

This work was supported by the National Science Foundation of China under Grants 62125206.

REFERENCES

- [1] M. Niknafs, I. Ukhov, P. Eles, and Z. Peng, "Runtime resource management with workload prediction," in *Annual Design Automation Conference 2019, DAC 2019*, 2019, pp. 1–6.
- [2] M. Babaioff, Y. Mansour, N. Nisan, G. Noti, C. Curino, N. Ganapathy, I. Menache, O. Reingold, M. Tennenholtz, and E. Timnat, "Era: A framework for economic resource allocation for the cloud," in *International Conference on World Wide Web Companion, WWW 2017*, 2017, p. 635–642.
- [3] J. Gao, H. Wang, and H. Shen, "Machine learning based workload prediction in cloud computing," in *International Conference on Computer Communications and Networks, ICCCN 2020*, 2020, pp. 1–9.
- [4] H. Moussa, I. Yen, F. B. Bastani, Y. Dong, and W. He, "Toward better service performance management via workload prediction," in *Services Computing - SCC 2019*, ser. Lecture Notes in Computer Science, vol. 11515, 2019, pp. 92–106.
- [5] Z. Chen, J. Hu, G. Min, A. Y. Zomaya, and T. A. El-Ghazawi, "Towards accurate prediction for high-dimensional and highly-variable cloud workloads with deep learning," *IEEE Trans. Parallel Distributed Syst.*, vol. 31, no. 4, pp. 923–934, 2020.
- [6] H. Aragon, S. Braganza, E. Boza, J. Parrales, and C. Abad, "Workload characterization of a software-as-a-service web application implemented with a microservices architecture," in *Companion Proceedings of The 2019 World Wide Web Conference, WWW 2019*, 2019, p. 746–750.
- [7] R. N. Calheiros, E. Masoumi, R. Ranjan, and R. Buyya, "Workload prediction using ARIMA model and its impact on cloud applications' qos," *IEEE Trans. Cloud Comput.*, vol. 3, no. 4, pp. 449–458, 2015.
- [8] Y. Jiang, M. Shahradd, D. Wentzlaff, D. H. K. Tsang, and C. Joe-Wong, "Burstable instances for clouds: Performance modeling, equilibrium analysis, and revenue maximization," *IEEE/ACM Trans. Netw.*, vol. 28, no. 6, pp. 2489–2502, 2020.
- [9] D. Ding, M. Zhang, X. Pan, M. Yang, and X. He, "Modeling extreme events in time series prediction," in *ACM SIGKDD International Conference on Knowledge Discovery & Data Mining, KDD 2019*, 2019, pp. 1114–1122.

- [10] Y. Zhu, W. Zhang, Y. Chen, and H. Gao, "A novel approach to workload prediction using attention-based LSTM encoder-decoder network in cloud environment," *EURASIP J. Wirel. Commun. Netw.*, vol. 2019, pp. 1–18, 2019.
- [11] H. Zhou, S. Zhang, J. Peng, S. Zhang, J. Li, H. Xiong, and W. Zhang, "Informer: Beyond efficient transformer for long sequence time-series forecasting," in *Conference on Artificial Intelligence, AAAI 2021*, 2021, pp. 11 106–11 115.
- [12] P. A. Dinda, "The statistical properties of host load," *Sci. Program.*, vol. 7, no. 3–4, pp. 211–229, 1999.
- [13] S. Guo, Y. Lin, N. Feng, C. Song, and H. Wan, "Attention based spatial-temporal graph convolutional networks for traffic flow forecasting," in *Conference on Artificial Intelligence, AAAI 2019*, 2019, pp. 922–929.
- [14] C. Chen, K. Li, S. G. Teo, X. Zou, K. Wang, J. Wang, and Z. Zeng, "Gated residual recurrent graph neural networks for traffic prediction," in *Conference on Artificial Intelligence, AAAI 2019*, 2019, pp. 485–492.
- [15] Z. Lv, J. Xu, K. Zheng, H. Yin, P. Zhao, and X. Zhou, "LC-RNN: A deep learning model for traffic speed prediction," in *Proceedings of International Joint Conference on Artificial Intelligence, IJCAI 2018*, 2018, pp. 3470–3476.
- [16] H. Yao, X. Tang, H. Wei, G. Zheng, and Z. Li, "Revisiting spatial-temporal similarity: A deep learning framework for traffic prediction," in *Conference on Artificial Intelligence, AAAI 2019*, 2019, pp. 5668–5675.
- [17] D. Ding, M. Zhang, X. Pan, M. Yang, and X. He, "Modeling extreme events in time series prediction," in *Proceedings of the 25th ACM SIGKDD International Conference on Knowledge Discovery & Data Mining*, 2019, pp. 1114–1122.
- [18] K. Cho, B. Van Merriënboer, C. Gulcehre, D. Bahdanau, F. Bougares, H. Schwenk, and Y. Bengio, "Learning phrase representations using rnn encoder-decoder for statistical machine translation," *arXiv preprint arXiv:1406.1078*, 2014.
- [19] A. Vaswani, N. Shazeer, N. Parmar, J. Uszkoreit, L. Jones, A. N. Gomez, L. Kaiser, and I. Polosukhin, "Attention is all you need," *Advances in neural information processing systems*, vol. 30, 2017.
- [20] S. Hochreiter and J. Schmidhuber, "Long short-term memory," *Neural Computation*, vol. 9, no. 8, pp. 1735–1780, 1997.
- [21] A. Vaswani, N. Shazeer, N. Parmar, J. Uszkoreit, L. Jones, A. N. Gomez, L. u. Kaiser, and I. Polosukhin, "Attention is all you need," in *Advances in Neural Information Processing Systems, NeurIPS 2017*, vol. 30, 2017.
- [22] J. Masci, U. Meier, D. Cireşan, and J. Schmidhuber, "Stacked convolutional auto-encoders for hierarchical feature extraction," in *Artificial Neural Networks and Machine Learning, ICANN 2011*. Springer Berlin Heidelberg, 2011, pp. 52–59.
- [23] H. Wu, J. Xu, J. Wang, and M. Long, "Autoformer: Decomposition transformers with auto-correlation for long-term series forecasting," in *Advances in Neural Information Processing Systems, NeurIPS 2021*, vol. 34, 2021, pp. 22 419–22 430.
- [24] N. Kitaev, L. Kaiser, and A. Levskaya, "Reformer: The efficient transformer," in *International Conference on Learning Representations, ICLR 2020*, 2020.
- [25] T. Zhou, Z. Ma, Q. Wen, X. Wang, L. Sun, and R. Jin, "Fedformer: Frequency enhanced decomposed transformer for long-term series forecasting," in *International Conference on Machine Learning, ICML 2022*, vol. 162, 2022, pp. 27 268–27 286.
- [26] Y. Su, Y. Zhao, C. Niu, R. Liu, W. Sun, and D. Pei, "Robust anomaly detection for multivariate time series through stochastic recurrent neural network," in *ACM SIGKDD international conference on knowledge discovery & data mining, KDD 2019*, 2019, pp. 2828–2837.
- [27] Q. Hu, P. Sun, S. Yan, Y. Wen, and T. Zhang, "Characterization and prediction of deep learning workloads in large-scale GPU datacenters," in *The International Conference for High Performance Computing, Networking, Storage and Analysis, SC '21*, 2021, pp. 104:1–104:15.
- [28] S. Xue, C. Qu, X. Shi, C. Liao, S. Zhu, X. Tan, L. Ma, S. Wang, S. Wang, Y. Hu *et al.*, "A meta reinforcement learning approach for predictive autoscaling in the cloud," in *ACM SIGKDD Conference on Knowledge Discovery and Data Mining, KDD 2022*, 2022, pp. 4290–4299.
- [29] Y. Zhang, W. Fan, X. Wu, H. Chen, B. Li, and M. Zhang, "CAFE: adaptive VDI workload prediction with multi-grained features," in *Artificial Intelligence, AAAI 2019*, 2019, pp. 5821–5828.
- [30] A. De Santo, A. Galli, M. Gravina, V. Moscato, and G. Sperli, "Deep learning for hdd health assessment: An application based on lstm," *IEEE Transactions on Computers*, vol. 71, no. 1, pp. 69–80, 2020.
- [31] L. Ma, D. Van Aken, A. Hefny, G. Mezerhane, A. Pavlo, and G. J. Gordon, "Query-based workload forecasting for self-driving database management systems," in *Proceedings of the 2018 International Conference on Management of Data*, 2018, pp. 631–645.
- [32] H. Chen, R. A. Rossi, K. Mahadik, S. Kim, and H. Eldardiry, "Graph deep factors for forecasting with applications to cloud resource allocation," in *ACM SIGKDD Conference on Knowledge Discovery & Data Mining, KDD 2021*, 2021, pp. 106–116.
- [33] C. Luo, B. Qiao, X. Chen, P. Zhao, R. Yao, H. Zhang, W. Wu, A. Zhou, and Q. Lin, "Intelligent virtual machine provisioning in cloud computing," in *International Joint Conference on Artificial Intelligence, IJCAI 2020*, 2020, pp. 1495–1502.
- [34] Y. Yao, D. Li, H. Jie, H. Jie, T. Li, J. Chen, J. Wang, F. Li, and Y. Gao, "Simplets: An efficient and universal model selection framework for time series forecasting," *Proceedings of the VLDB Endowment*, vol. 16, no. 12, pp. 3741–3753, 2023.
- [35] M. Stockman, M. Awad, H. Akkary, and R. Khanna, "Thermal status and workload prediction using support vector regression," in *International Conference on Energy Aware Computing*, 2012, pp. 1–5.
- [36] P. Singh, P. Gupta, and K. Jyoti, "TASM: technocrat ARIMA and SVR model for workload prediction of web applications in cloud," *Clust. Comput.*, vol. 22, no. 2, pp. 619–633, 2019.
- [37] W. Zhang, B. Li, D. Zhao, F. Gong, and Q. Lu, "Workload prediction for cloud cluster using a recurrent neural network," in *International Conference on Identification, Information and Knowledge in the Internet of Things (IIKI)*, 2016, pp. 104–109.
- [38] J. Kumar, R. Goomer, and A. K. Singh, "Long short term memory recurrent neural network (lstm-rnn) based workload forecasting model for cloud datacenters," *Procedia Computer Science*, vol. 125, pp. 676–682, 2018.
- [39] A. Bauer, M. Züfle, N. Herbst, S. Kounev, and V. Curtef, "Telescope: An automatic feature extraction and transformation approach for time series forecasting on a level-playing field," in *2020 IEEE 36th International Conference on Data Engineering (ICDE)*, 2020, pp. 1902–1905.
- [40] Y. Liang, S. Ke, J. Zhang, X. Yi, and Y. Zheng, "Geoman: Multi-level attention networks for geo-sensory time series prediction," in *International conference on international joint conferences on artificial intelligence, IJCAI 2018*, 2018, pp. 3428–3434.
- [41] W. Li, R. Bao, K. Harimoto, D. Chen, J. Xu, and Q. Su, "Modeling the stock relation with graph network for overnight stock movement prediction," in *International conference on international joint conferences on artificial intelligence, IJCAI 2021*, 2021, pp. 4541–4547.
- [42] R.-G. Cirstea, T. Kieu, C. Guo, B. Yang, and S. J. Pan, "Enhancenet: Plugin neural networks for enhancing correlated time series forecasting," in *2021 IEEE 37th International Conference on Data Engineering (ICDE)*, 2021, pp. 1739–1750.
- [43] Y. Cui, K. Zheng, D. Cui, J. Xie, L. Deng, F. Huang, and X. Zhou, "Metro: a generic graph neural network framework for multivariate time series forecasting," *Proceedings of the VLDB Endowment*, vol. 15, no. 2, pp. 224–236, 2021.
- [44] X. Wu, D. Zhang, C. Guo, C. He, B. Yang, and C. S. Jensen, "Autocts: Automated correlated time series forecasting," *Proceedings of the VLDB Endowment*, vol. 15, no. 4, pp. 971–983, 2021.
- [45] T. Belkhouja, Y. Yan, and J. R. Doppa, "Training robust deep models for time-series domain: Novel algorithms and theoretical analysis," in *Proceedings of the AAAI Conference on Artificial Intelligence*, vol. 36, no. 6, 2022, pp. 6055–6063.
- [46] Q. Tan, M. Ye, B. Yang, S. Liu, A. J. Ma, T. C.-F. Yip, G. L.-H. Wong, and P. Yuen, "Data-gru: Dual-attention time-aware gated recurrent unit for irregular multivariate time series," in *Proceedings of the AAAI Conference on Artificial Intelligence*, vol. 34, no. 01, 2020, pp. 930–937.
- [47] X. Zhang, Y. Gao, J. Lin, and C.-T. Lu, "Tapnet: Multivariate time series classification with attentional prototypical network," in *Proceedings of the AAAI Conference on Artificial Intelligence*, vol. 34, no. 04, 2020, pp. 6845–6852.
- [48] X. Tang, H. Yao, Y. Sun, C. Aggarwal, P. Mitra, and S. Wang, "Joint modeling of local and global temporal dynamics for multivariate time series forecasting with missing values," in *Proceedings of the AAAI Conference on Artificial Intelligence*, vol. 34, no. 04, 2020, pp. 5956–5963.
- [49] Y. Luo, Y. Zhang, X. Cai, and X. Yuan, "E2gan: End-to-end generative adversarial network for multivariate time series imputation," in *Proceedings of the 28th international joint conference on artificial intelligence*. AAAI Press, 2019, pp. 3094–3100.